Warren N. White
Assoc. Professor,
Assoc. Mem. ASME.

Srinivasan Venkatasubramanian
Graduate Student.

Mechanical Engineering Department,
Kansas State University,
Manhattan, KS 66506-5106

P. Michael Lynch
Professor,
Mechanical Engineering Department,
Tulane University,
New Orleans, LA 70118
Mem. ASME.

Chi-Lung D. Huang
Professor,
Mechanical Engineering Department,
Kansas State University,
Manhattan, KS 66506-5106
Mem. ASME.

The Equations of Motion for the Torsional and Bending Vibrations of a Stranded Cable

Equations of motion of a thin, stranded elastic cable with an eccentric, attached mass and subject to aerodynamic loading are derived using Hamilton's principle. Coupling between the translational and rotational degrees of freedom owing to inertia, elasticity, and stranded geometry are considered. By invoking simplifying assumptions, the equations of motion are reduced to those obtained previously by other researchers.

Introduction

A cable in the form of a catenary is found in many engineering structures such as suspension bridges, aerial transmission lines, and underwater anchors for deep sea drilling platforms to name just a few. One underlying similarity among these mechanical structures is that the cable is intended to remain static. Motion of the cable is then of concern since this represents a departure from the intended state in which the structure would be employed. By understanding the cable dynamics, engineers are able to either accommodate the cable motion or seek suitable ways to quench or limit its oscillation.

A significant problem concerning the oscillation of the cable is that of the galloping of aerial transmission lines. Galloping, which is a low-frequency, high-amplitude oscillation, has been a concern for many decades for overhead electric power transmission line designers. Transmission line galloping occurs when ice or freezing precipitation adheres to a power line conductor. Owing to the ice build up, the cross-section of the conductor becomes noncircular. A noncircular profile gives the conductor both aerodynamic lift and drag characteristics. Aerodynamic lift force can give rise to dynamic instability even at low wind speeds. When conditions are suitable for dynamic instability, spectacularly large-amplitude, low-frequency mechanical vibration of the line occurs. Since galloping can cause various kinds of structural damage and power outages, each having its own associated cost and problems, many attempts have been made to stop galloping or at least minimize its amplitude. In order to design a better preventative or damping mechanism, a knowledge of the mechanics of galloping is required.

A history of the means by which cable motion has been described begins with the wave equation which applies to any thin cable of symmetric cross-section in which both the tension and axial strain are constant. Routh (1905) presented the equations of motion of an inelastic chain having symmetric cross-section (cable cross-sectional mass center coincides with the cable center). However, the mass per unit length in the example in Routh's text was sufficient so that the constant tension assumption was invalid. Also, only the in-plane motions were considered in Routh's analysis. The solution of the static inelastic chain equations is the familiar catenary shape. Cheers (1950) used a small perturbation analysis for the cable motion which resulted in wave equation analysis. Equations of motion for an elastic cable of symmetric cross-section were presented by Shea (1955) and by Simpson (1963). The equations of motion, presented by Shea and Simpson, assume an absence of torsional motion. In both of these investigations, motion of

Contributed by the ASME Applied Mechanics Division of THE AMERICAN SOCIETY OF MECHANICAL ENGINEERS for presentation at the Winter Annual Meeting, Atlanta, Ga., Dec. 1-6, 1991.

Discussion on this paper should be addressed to the Technical Editor, Prof. Leon M. Keer, The Technological Institute, Northwestern University, Evanston, IL 60208, and will be accepted until two months after final publication of the paper itself in the JOURNAL OF APPLIED MECHANICS. Manuscript received by the ASME Applied Mechanics Division, Nov. 15, 1990; final revision, Apr. 25, 1991.

Paper No. 91-WA/APM-19.

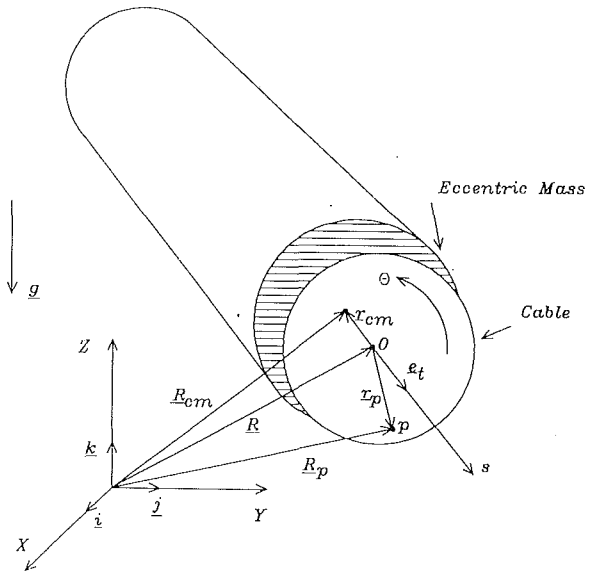

Fig. 1 Conductor geometry

the cable in all three Cartesian coordinates was considered.

In what appears to be the first work regarding the torsional motion of the conductor, Simpson (1972) presented equations of motion for a bundled conductor. These equations of Simpson governed the three Cartesian directions of motion as well as the axial twist. Thompson (1975) also considered the torsional motion of a single conductor with the added assumption that no motion takes place in the cable axial direction.

The bundled conductor work of Simpson (1972) included bending stresses. In most work involving single conductor motion, bending stresses have been excluded from consideration owing to the small cable radius and the large radius of the curvature of the line. An exception to this is Cheers (1950). Since the radius of the conductor bundle is much larger than the radius of a single conductor, bending stresses now become significant. Gawronski (1977) also treated bundled conductors; however, the axis of bending was assumed to pass through both conductors of his two conductor bundle which indicates that the bending stresses would not be greater than that found on a single conductor span. Gawronski was first to consider an axial-torsional coupling which linked the axial tension to the determination of torsional stiffness of the bundle.

In this paper, the equations of motion of a single conductor span having an eccentric mass attached to the cable which provides no additional strength to the line are derived through Hamilton's principle. Validity of the equations will be checked through a virtual work argument. By invoking additional assumptions such as the absence of ice, shallow catenary, and the lack of torsional motion, it is possible to compare the work presented here to the results produced by others. It will be seen that a term will appear in the equations of motion which is new to the galloping mechanics literature. This new term demonstrates that the torsional motion and the Cartesian motion are coupled together even if there is no ice on the line. This new term stems from a constraint upon conductor orientation which reduces the number of degrees-of-freedom for motion of a differential portion of the cable from six to four, namely three Cartesian directions and axial twist.

Mechanical Analysis

The analysis of a galloping line begins with the presentation of the assumptions made in the derivation of the dynamic equations. The equations of motion will be determined by setting the first variation of the Lagrangian of the translating and rotating cable equal to the applied excitations. In order to facilitate the calculation of the kinetic and potential energies

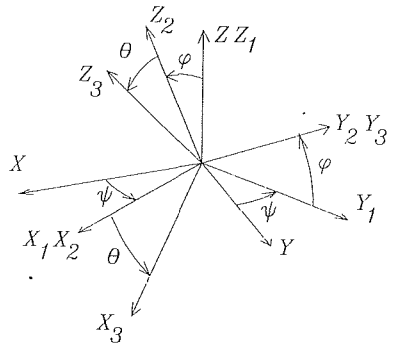

Fig. 2 Euler angle definitions

necessary to construct the Lagrangian, two coordinate systems will be used. These coordinate systems and the transformations between these frames will be presented. While the calculation of the Lagrangian component energies is an application of familiar procedures, determination of the first variation involves considerable effort. At this point of the analysis, detailed steps of the computation of the first variation will be given. The analysis section will then conclude with the dynamic equations.

Assumptions. Governing equations of motion for a galloping cable are derived in accordance with several assumptions. All of these assumptions pertain either to mechanics of conductor motion or the materials and shapes peculiar to galloping cables. These assumptions are as follows:

1 The cable is an elastic string with constant mass per unit length and circular cross-section.
2 The material used in the cable construction is isotropic with constant material properties.
3 Bending stresses in a single conductor span are small owing to the large radius of curvature of the cable.
4 Mass per unit length, cross-sectional area, shape, and angle of deposit of the eccentric mass is constant along the length of the cable.
5 The only source of damping present in the mechanical system comes from wind drag. No damping forces arise from elastic hysteresis or relative conductor strand movement.
6 The eccentric mass provides no additional axial, torsional, or bending stiffness to the cable.

Coordinate Systems. The analysis will make use of two separate coordinate systems. Motion of the conductor center is described with respect to a frame fixed in space. Attached to the conductor center is a local frame which translates and rotates with respect to the fixed or global frame. The local, conductor centered frame is used to describe both the orientation of the conductor cross-section and the angle of twist of the cable. The transformation between the fixed frame and the local frame is described in terms of Euler angles.

Figure 1 illustrates the global coordinate system and a cross-section of the aerial conductor. Vectors $\mathbf{R}$ and $\mathbf{R}_{cm}$ denote the position, with respect to the global frame, of the conductor center and the cross-sectional mass center, respectively. Vector $\mathbf{r}_{cm}$ denotes the mass center with respect to the conductor center, O. Vector $\mathbf{e}_t$ is a unit vector tangent to the cable. Each of the vectors $\mathbf{R}$, $\mathbf{R}_{cm}$, $\mathbf{r}_{cm}$, and $\mathbf{e}_t$ are functions of the scalar parameter s which measures unstressed distance along the conductor. The angle of twist of the cable is the angle θ. The point p is an arbitrary point on the cable cross-section.

The three Euler angles ψ, ϕ, and θ describing the rotational transformation between the global frame and the local frame are illustrated in Fig. 2. The transformation is accomplished by first rotating about the global Z axis by ψ to produce the X_1, Y_1, Z_1 frame. A rotation about the X_1-axis by ϕ produces the frame X_2, Y_2, Z_2. The coordinate frame determined by X_2,

Y_2, Z_2 is important to the analysis since the X_2-Z_2 plane constitutes the conductor cross-section. The angle θ (which is the final Euler angle) measures conductor twist about the Y_2 axis, and the Y_2 (and Y_3) axis is parallel to the conductor unit tangent vector $\mathbf{e}_t$. Details of the transformations will be included in the analysis as needed.

The Lagrangian. Coordinate systems previously presented will now be used to develop expressions for the kinetic, gravitational potential, and elastic strain energies necessary to form the Lagrangian.

Kinetic Energy. We will now determine the kinetic energy of a translating and rotating cable with an eccentric additional mass. Referring to Fig. 1, consider an arbitrary particle p on the conductor cross-section. The position vector to that particle with respect to the global coordinate system is

$$\mathbf{R}_p = \mathbf{R} + \mathbf{r}_p \tag{1}$$

where $\mathbf{r}_p$ is the position of the particle with respect to the conductor center. The velocity of the particle in the fixed frame is given by

$$\mathbf{V}_p = \dot{\mathbf{R}} + \omega \times \mathbf{r}_p = \mathbf{V} + \omega \times \mathbf{r}_p \tag{2}$$

where $\mathbf{V}$ is the velocity of the cable center in the global frame and the dot represents differentiation with respect to time. The vector ω is the angular velocity of the conductor as seen by an observer in the fixed frame. The kinetic energy, KE_p, of this particle which has mass m_p, is

$$KE_p = \frac{1}{2} m_p |\mathbf{V}_p|^2. \tag{3}$$

The kinetic energy, KE, of a unit length of line is

$$KE = \sum_p \frac{1}{2} m_p |\mathbf{V}_p|^2 \tag{4}$$

where the sum is computed over all particles composing a unit length of the cable. Carrying out the operation of Eq.(4) produces

$$KE = \frac{1}{2}\sum_p m_p |\mathbf{V}|^2 + \mathbf{V}\cdot(\omega \times \sum_p m_p \mathbf{r}_p) + \frac{1}{2}\sum_p m_p (\omega \times \mathbf{r}_p)^2$$

$$= \frac{1}{2} m |\mathbf{V}|^2 + m\,\mathbf{V}\cdot(\omega \times \mathbf{r}_{cm}) + \frac{1}{2}\sum_{i,j} I_{ij}\omega_i\omega_j \tag{5}$$

where m is the total cable mass per unit unstressed length determined by

$$m = \sum_p m_p \tag{6}$$

and where I_{ij} are inertia tensor components computed as

$$I_{ij} = \sum_p m_p [\delta_{ij} |\mathbf{r}_p|^2 - r_{p_i} r_{p_j}]. \tag{7}$$

Note that δ_{ij} is the Kronecker delta and that r_{p_i} and r_{p_j} are components of the vector $\mathbf{r}_p$. Likewise, ω_i and ω_j are components of the angular velocity ω. Futhermore, it should be noted that all vector quantities in (5) are expressed in the fixed frame.

The total kinetic energy of the line, KE_T, is determined by integrating (5) over the length of the line to yield

$$KE_T = \frac{m}{2}\int_0^{FL} |\dot{\mathbf{R}}|^2 ds + m\int_0^{FL} \dot{\mathbf{R}}\cdot(\omega \times \mathbf{r}_{cm}) ds$$

$$+ \frac{1}{2}\int_0^{FL}\int_{A_T} \rho(\omega \times \mathbf{r}_p)\cdot(\omega \times \mathbf{r}_p) dA\, ds \tag{8}$$

where FL is the free, unstressed length of the line, A_T is the total cross-sectional region of the line including eccentric mass, and ρ is the mass density which varies over the cross-section.

Potential Energy. The potential energy is divided into two parts which consist of the gravitational potential energy and the elastic strain energy. We will treat each part separately.

Gravitational Potential Energy. The gravitational potential energy is

$$PE_g = -m\,\mathbf{g}\cdot\int_0^{FL} (\mathbf{R} + \mathbf{r}_{cm}) ds \tag{9}$$

where $\mathbf{g}$ is the gravitational acceleration vector.

Elastic Strain Energy. The total elastic strain energy of the line is determined by integrating the strain energy density over the entire region of the conductor. Before this can be accomplished, both the axial and torsional strains and the accompanying stresses must be expressed in terms of the conductor displacements. To this end we adopt the constitutive relation presented by McConnell and Zemke (1976) which, for the purposes of this work, is

$$P = AE\epsilon + B\frac{\partial\theta}{\partial s} \tag{10}$$

for the axial tension P and

$$T = B\epsilon + JG\frac{\partial\theta}{\partial s} \tag{11}$$

for the torsion T. In (10) and (11), AE and JG are the axial and torsional stiffness of the cable, respectively. A is the cross-sectional area of the bare, unstressed cable. B represents the coupling between axial and torsional displacements owing to the stranded, wound nature of the cable construction. The axial strain ϵ is

$$\epsilon = \left|\frac{\partial \mathbf{R}}{\partial s}\right| - 1. \tag{12}$$

The constitutive model gives the strain energy as

$$SE = \frac{1}{2}\int_0^{FL} P\epsilon\, ds + \frac{1}{2}\int_0^{FL} T\frac{\partial\theta}{\partial s} ds$$

$$= \frac{1}{2}\int_0^{FL} \begin{bmatrix} \epsilon & \dfrac{\partial\theta}{\partial s} \end{bmatrix} \begin{bmatrix} AE & B \\ B & JG \end{bmatrix} \begin{bmatrix} \epsilon \\ \dfrac{\partial\theta}{\partial s} \end{bmatrix} ds. \tag{13}$$

By combining the results of (8), (9), and (13), we can write the Lagrangian, L, of the line as

$$L(\mathbf{R}, \dot{\mathbf{R}}, \mathbf{R}_s, \dot{\mathbf{R}}_s, \theta, \dot{\theta}, \theta_s) = KE_T - PE_g - SE \tag{14}$$

where the subscript s denotes partial differentiation with respect to s.

The First Variation. Equations of motion for the cable originate from the determination of the first variation of (14). This process will produce a coupled system of one vector equation and one scalar equation for determination of cable displacement $\mathbf{R}$ and twist θ. We will consider each of the component energies in turn beginning with the potential energies and concluding with the kinetic energy.

Gravitational Potential Energy. The variation of the gravitational potential energy arises because of cable displacement and rotation. The first variation of PE_g is

$$\delta PE_g = -m\mathbf{g}\cdot\int_0^{FL}\left[\frac{\partial}{\partial \mathbf{R}}(\mathbf{R} + \mathbf{r}_{cm})\delta\mathbf{R} + \frac{\partial}{\partial\theta}(\mathbf{R} + \mathbf{r}_{cm})\delta\theta\right] ds$$

$$= -m\mathbf{g}\cdot\int_0^{FL} [\delta\mathbf{R} + (\delta\beta \times \mathbf{r}_{cm})] ds$$

$$= -m\mathbf{g}\cdot\int_0^{FL} \delta\mathbf{R}\, ds - \int_0^{FL} (\mathbf{r}_{cm} \times m\mathbf{g})\cdot\delta\beta\, ds. \tag{15}$$

where $\delta\beta$ is a rotational or pseudo vector formed by variations in the three Euler angles. The terms on the right side of (15)

will eventually contribute a gravitational force and a gravitational moment about the conductor center.

The vector $\delta\beta$ is readily obtained from the Euler transformation itself. Let $\mathbf{r}_p'$ be an arbitrary vector in the local frame. The corresponding representation in the global frame is the vector $\mathbf{r}_p$ given by

$$\begin{aligned}\mathbf{r}_p &= [\Gamma]\mathbf{r}_p' \\ &= [Rot(Z,\ \psi)][Rot(X_1,\ \phi)][Rot(Y_2,\ \theta)]\mathbf{r}_p' \end{aligned} \tag{16}$$

where $[Rot(w,\ v)]$ represents a rotation matrix formed by a rotation of angle v in the right-handed sense about axis w and $[\Gamma]$ is the Euler angle transformation which converts vectors from representation in the local frame to their representation in the fixed frame. The variation of $\mathbf{r}_p$ with respect to the Euler angles is given by

$$\begin{aligned}\delta\mathbf{r}_p &= \left\{\frac{\partial}{\partial\psi}[\Gamma]\delta\psi + \frac{\partial}{\partial\phi}[\Gamma]\delta\phi + \frac{\partial}{\partial\theta}[\Gamma]\delta\theta\right\}[\Gamma]^T\mathbf{r}_p \\ &= \delta\beta\times\mathbf{r}_p \end{aligned} \tag{17}$$

where the superscript T denotes matrix transpose. The result of the differentiation and matrix multiplication in (17) produces the pseudo vector $\delta\beta$ which is given by

$$\delta\beta = \delta\psi\mathbf{k} + \delta\phi\hat{\mathbf{X}}_1 + \delta\theta\mathbf{e}_t = [D]\delta\Lambda \tag{18}$$

where $\hat{\mathbf{X}}_1$ is a unit vector which points along the X_1-axis of Fig. 2. Note that by employing the same algebraic steps we could consider the time derivative of $\mathbf{r}_p$, a process which leads to the angular velocity pseudo-vector ω given by

$$\omega = \dot{\beta} = \dot{\psi}\mathbf{k} + \dot{\phi}\hat{\mathbf{X}}_1 + \dot{\theta}\mathbf{e}_t = [D]\dot{\Lambda}. \tag{19}$$

Here, $[D]$ is the matrix

$$[D] = [\mathbf{k}\ \hat{\mathbf{X}}_1\ \mathbf{e}_t] \tag{20}$$

and Λ is the column vector

$$\Lambda = [\psi\ \phi\ \theta]^T. \tag{21}$$

Strain Energy. By determining the first variation of the strain energy, we will recover expressions which contain the axial and torsional stiffness terms. The variation of the strain energy is found, after setting the first variation of $\mathbf{R}$ and θ at the ends of the line to zero, as

$$\delta SE = \int_0^{FL}\left[\frac{\partial}{\partial s}\left(\frac{P}{1+\epsilon}\frac{\partial\mathbf{R}}{\partial s}\right)\cdot\delta\mathbf{R} + \frac{\partial}{\partial s}(T)\delta\theta\right]ds. \tag{22}$$

Kinetic Energy. The task remaining in finding the first variation is the consideration of the kinetic energy. Its variation is

$$\begin{aligned}\delta\int_{t_1}^{t_2} KE_T dt = \delta\int_{t_1}^{t_2}\int_0^{FL}\frac{1}{2}m\dot{\mathbf{R}}\cdot\dot{\mathbf{R}}dsdt \\ + \delta\int_{t_1}^{t_2}\int_0^{FL}\int_{A_T}\rho\dot{\mathbf{R}}\cdot(\omega\times\mathbf{r}_p)dAdsdt \\ + \delta\int_{t_1}^{t_2}\int_0^{FL}\int_{A_T}\frac{\rho}{2}(\omega\times\mathbf{r}_p)\cdot(\omega\times\mathbf{r}_p)dAdsdt. \end{aligned} \tag{23}$$

After computing the variation, integrating by parts, and finally setting the variations of $\mathbf{R}$ at either end point in time to zero, the first term on the right of (23) becomes

$$\delta\int_{t_1}^{t_2}\int_0^{FL}\frac{1}{2}m\dot{\mathbf{R}}\cdot\dot{\mathbf{R}}\ dsdt = -\int_{t_1}^{t_2}\int_0^{FL} m\ddot{\mathbf{R}}\cdot\delta\mathbf{R}\ dsdt. \tag{24}$$

The next two terms can be manipulated into the intermediate form of

$$\begin{aligned}\delta\int_{t_1}^{t_2}\int_0^{FL}\int_{A_T}\rho\left[\dot{\mathbf{R}}\cdot(\omega\times\mathbf{r}_p) + \frac{1}{2}(\omega\times\mathbf{r}_p)\cdot(\omega\times\mathbf{r}_p)\right]dAdsdt \\ = -\int_{t_1}^{t_2}\int_0^{FL} m(\alpha\times\mathbf{r}_{cm} + \omega\times(\omega\times\mathbf{r}_{cm}))\cdot\delta\mathbf{R}\ dsdt \\ + \int_{t_1}^{t_2}\int_0^{FL}\int_{A_T}\rho(\mathbf{r}_p\times(\ddot{\mathbf{R}} + (\omega\times\mathbf{r}_p)))\cdot\delta\omega\ dAdsdt \\ + \int_{t_1}^{t_2}\int_0^{FL}\int_{A_T}\rho(\mathbf{r}_p\times((\ddot{\mathbf{R}} + \omega\times\mathbf{r}_p)\times\omega))\cdot\delta\beta\ dAdsdt. \end{aligned} \tag{25}$$

The first term on the right of (25) is in the desired form; the last two terms require further attention.

At this point of the derivation there are two directions which we can follow. The first is to write the variation of ω as

$$\delta\omega = \frac{\partial\omega}{\partial\dot{\Lambda}}\delta\dot{\Lambda} + \frac{\partial\omega}{\partial\Lambda}\delta\Lambda \tag{26}$$

which is the most direct way. The other path requires that we realize that

$$\frac{d}{dt}(\delta\beta) = \delta\dot{\beta} + \omega\times\delta\beta. \tag{27}$$

Now, (27) can be most easily verified by directly substituting the various quantities. The form of (27) arises since the last two Euler angles represent rotations around unit vectors which are themselves rotating. From (27) we now recognize that

$$\delta\dot{\beta} = \delta\omega = \frac{d}{dt}(\delta\beta) - \omega\times\delta\beta. \tag{28}$$

In completing the determination of the variations in (25) we can use either (26) or (28) to arrive at the same result; however, the algebraic complexity of using (28) is considerably less than the alternative.

After substituting (28) into (25), integrating by parts, substituting the definitions of the inertia tensor and the center of mass, simplifying, and combining the end result with (24), the variation of the kinetic energy with respect to $\mathbf{R}$ and the Euler angles becomes

$$\begin{aligned}\delta\int_{t_1}^{t_2} KE_T dt = -\int_{t_1}^{t_2}\int_0^{FL}[m(\ddot{\mathbf{R}} + \alpha\times\mathbf{r}_{cm} + \omega\times(\omega\times\mathbf{r}_{cm}))\cdot\delta\mathbf{R} \\ + (\mathbf{r}_{cm}\times m\ddot{\mathbf{R}} + I\alpha + \omega\times I\omega)\cdot\delta\beta]dsdt. \end{aligned} \tag{29}$$

In order to finish this step we must expand $\delta\beta$ in terms of line displacement and twist.

Determining the variation $\delta\beta$ as a function of the variations $\delta\theta$ and $\delta\mathbf{R}_s$ is facilitated by using (18). This process produces

$$\delta\beta = [D]\delta\Lambda = [D]\frac{\partial\Lambda}{\partial\mathbf{R}_s}\delta\mathbf{R}_s + \mathbf{e}_t\delta\theta. \tag{30}$$

In order to evaluate the derivative $\partial\Lambda/\partial\mathbf{R}_s$ we note that the unit tangent to the line can be written as

$$\mathbf{e}_t = -\sin\psi\cos\phi\,\mathbf{i} + \cos\psi\cos\phi\,\mathbf{j} + \sin\phi\,\mathbf{k} = \frac{1}{1+\epsilon}\frac{\partial\mathbf{R}}{\partial s}. \tag{31}$$

By equating components and computing differentials then it is possible, after considerable algebra, to demonstrate that

$$\frac{\partial\psi}{\partial\mathbf{R}_s} = -\frac{\hat{\mathbf{X}}_1^T}{(X_s^2 + Y_s^2)^{1/2}} \tag{32}$$

and

$$\frac{\partial\phi}{\partial\mathbf{R}_s} = \hat{\mathbf{Z}}_2^T\frac{1}{1+\epsilon} \tag{33}$$

where $\hat{\mathbf{Z}}_2$ is a unit vector along the Z_2-axis of Fig. 2. Substituting (32) and (33) into (30) finally produces

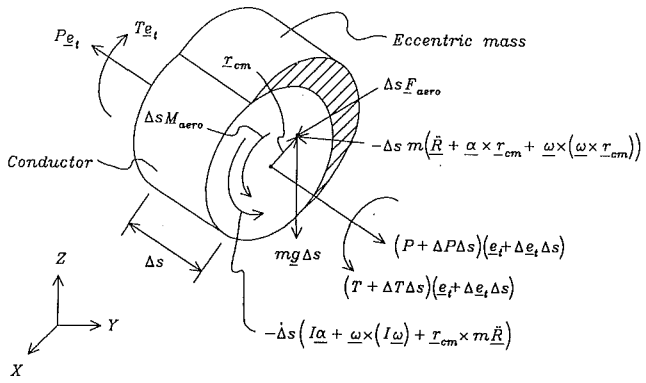

Fig. 3 Cable loading with elastic, external, and inertial forces

$$\delta\beta = \frac{1}{1+\epsilon}\left[\hat{\mathbf{X}}_1\,\hat{\mathbf{Z}}_2^T - \mathbf{k}\,\hat{\mathbf{X}}_1^T\frac{(1+\epsilon)}{(X_s^2+Y_s^2)^{1/2}}\right]\delta\mathbf{R}_s + \mathbf{e}_t\delta\theta. \quad (34)$$

We can now complete the first variation of the kinetic energy by substituting (34) into (29), integrating by parts, and setting the first variation of $\mathbf{R}$ at the ends of the line to zero. Doing this gives

$$\delta\int_{t_1}^{t_2} KE_T\,dt = \int_{t_1}^{t_2}\int_0^{FL}\left\{\left[-m(\ddot{\mathbf{R}} + \boldsymbol{\alpha}\times\mathbf{r}_{cm} + \boldsymbol{\omega}\times(\boldsymbol{\omega}\times\mathbf{r}_{cm})) + \frac{\partial}{\partial s}\left(\frac{1}{1+\epsilon}\left(-\mathbf{r}_{cm}\times m\ddot{\mathbf{R}} - I\boldsymbol{\alpha} - \boldsymbol{\omega}\times(I\boldsymbol{\omega})\right)^T \cdot\left[\mathbf{k}\,\hat{\mathbf{X}}_1^T\frac{1+\epsilon}{(X_s^2+Y_s^2)^{1/2}} - \hat{\mathbf{X}}_1\,\hat{\mathbf{Z}}_2^T\right]\right)\right]\cdot\delta\mathbf{R} + [(-\mathbf{r}_{cm}\times m\ddot{\mathbf{R}} - I\boldsymbol{\alpha} - \boldsymbol{\omega}\times(I\boldsymbol{\omega}))\cdot\mathbf{e}_t]\delta\theta\right\} ds\,dt. \quad (35)$$

The Equations of Motion. By equating the variations of the Lagrangian with respect to $\mathbf{R}$ and θ to the virtual work done by these external excitations, which are not represented through a potential, we produce the equations of motion. These are given by

$$m(\ddot{\mathbf{R}} + \boldsymbol{\alpha}\times\mathbf{r}_{cm} + \boldsymbol{\omega}\times(\boldsymbol{\omega}\times\mathbf{r}_{cm})) = \mathbf{F}_{\text{aero}} + m\mathbf{g} + \frac{\partial}{\partial s}\left\{\frac{1}{1+\epsilon}\left[P\frac{\partial\mathbf{R}}{\partial s} + \left(\hat{\mathbf{X}}_1\mathbf{k}^T\frac{(1+\epsilon)}{(X_s^2+Y_s^2)^{1/2}} - \hat{\mathbf{Z}}_2\,\hat{\mathbf{X}}_1^T\right)\cdot(\mathbf{r}_{cm}\times m\mathbf{g} - \mathbf{r}_{cm}\times m\ddot{\mathbf{R}} - I\boldsymbol{\alpha} - \boldsymbol{\omega}\times(I\boldsymbol{\omega}))\right]\right\} \quad (36)$$

and

$$(\mathbf{r}_{cm}\times m\mathbf{g} - \mathbf{r}_{cm}\times m\ddot{\mathbf{R}} - I\boldsymbol{\alpha} - \boldsymbol{\omega}\times(I\boldsymbol{\omega}))\cdot\mathbf{e}_t + \frac{\partial T}{\partial s} = -M_{\text{aero}} \quad (37)$$

where $\mathbf{F}_{\text{aero}}$ and M_{aero} are the external aerodynamic force and pitching moment, respectively.

Verification. As an independent means of verifying the equations of motion, we use the principle of virtual work. The procedure to be followed is to consider the sum of the elastic, inertial, and gravitational forces and moments acting on a section of cable. The work done by the net force and moment in moving the entire cable through a virtual displacement $\delta\mathbf{R}$ and $\delta\beta$, a displacement consistent with the constraints, is then set to zero. By factoring the various components of the virtual displacement, namely, δX, δY, δZ, and $\delta\theta$ and by noting that these displacements are independent, the equations of motion are obtained.

Figure 3 shows a small portion of cable with internal, external, and inertial loadings. The net force and moment will now be considered. Summing forces and ignoring the products of small terms provides

$$\sum\mathbf{F} = \Delta s[\Delta(P\mathbf{e}_t) + m\mathbf{g} + \mathbf{F}_{\text{aero}} - m(\ddot{\mathbf{R}} + \boldsymbol{\alpha}\times\mathbf{r}_{cm} + \boldsymbol{\omega}\times(\boldsymbol{\omega}\times\mathbf{r}_{cm}))]. \quad (38)$$

The moment sum is

$$\sum\mathbf{M} = \Delta s[\Delta(T\mathbf{e}_t) + \mathbf{M}_{\text{aero}} + \mathbf{r}_{cm}\times m\mathbf{g} - (I\boldsymbol{\alpha} + \boldsymbol{\omega}\times(I\boldsymbol{\omega}) + \mathbf{r}_{cm}\times m\ddot{\mathbf{R}})]. \quad (39)$$

By letting Δs shrink to differential proportions, we can then compute the work, δW, done through a virtual displacement as

$$\delta W = \int_0^{FL}\left(\sum\mathbf{F}\cdot\delta\mathbf{R} + \sum\mathbf{M}^T\delta\boldsymbol{\beta}\right)ds. \quad (40)$$

The constraint on the motion given by

$$\delta\boldsymbol{\beta} = \frac{\partial\boldsymbol{\beta}}{\partial\mathbf{R}_s}\delta\mathbf{R}_s + \delta\theta\mathbf{e}_t \quad (41)$$

is now included. By substituting (41) into (40), integrating by parts, and finally setting the virtual displacement $\delta\mathbf{R}$ at the end points to zero, produces

$$\delta W = \int_0^{FL}\left[\left(\sum\mathbf{F} - \frac{\partial}{\partial s}\left(\sum\mathbf{M}^T\frac{\partial\boldsymbol{\beta}}{\partial\mathbf{R}_s}\right)\right)\cdot\delta\mathbf{R} + \sum\mathbf{M}\cdot\mathbf{e}_t\delta\theta\right]ds. \quad (42)$$

Since the displacements are consistent with the constraints, the virtual work vanishes. The displacements $\delta\mathbf{R}$ and $\delta\theta$ are independent and arbitrary. The independence of the virtual displacements leads to the conclusion

$$\sum\mathbf{F}^T - \frac{\partial}{\partial s}\left(\sum\mathbf{M}^T\frac{\partial\boldsymbol{\beta}}{\partial\mathbf{R}_s}\right) = 0 \quad (43)$$

and

$$\sum\mathbf{M}\cdot\mathbf{e}_t = 0 \quad (44)$$

which produces the original Eqs. (36) and (37).

Comparisons With Previous Work

Comparisons of the equations of motion given in (36) and (37) with results of other investigators are possible provided additional assumptions are made. It is instructive to see what additional assumptions are necessary in order to match the results of others since this provides an understanding of the assumption influence upon the equations of motion.

Shallow Catenary Assumption. The first assumption to be invoked is that the sag-to-span ratio is small. The implication of this assumption is that the unit tangent to the line is everywhere horizontal and can be made to coincide with one of the fixed frame axes. Making the Y-axis coincide with the line means that the vector $\mathbf{r}_{cm}$ is contained in the X-Z plane. Another influence of this assumption is that all torsional motion is about the Y-axis exclusively.

Under this assumption the equations of motion simplify significantly. The translational part of the motion is governed by

$$m(\ddot{\mathbf{R}} + \ddot{\theta}\mathbf{j}\times\mathbf{r}_{cm} - \dot{\theta}^2\mathbf{r}_{cm}) = \mathbf{F}_{\text{aero}} + m\mathbf{g} + \frac{\partial}{\partial s}\left(\frac{1}{1+\epsilon}\left[P\frac{\partial\mathbf{R}}{\partial s} - \left(\mathbf{i}\,\mathbf{k}^T\frac{(1+\epsilon)}{|Y_s|} - \mathbf{k}\,\mathbf{i}^T\right)\cdot(\mathbf{r}_{cm}\times m\ddot{\mathbf{R}})\right]\right) \quad (45)$$

while the torsional equation becomes

$$(\mathbf{r}_{cm}\times m\mathbf{g} - \mathbf{r}_{cm}\times m\ddot{\mathbf{R}} - I\ddot{\theta}\mathbf{e}_t)\cdot\mathbf{e}_t + \frac{\partial T}{\partial s} = -M_{\text{aero}}. \quad (46)$$

If we make the additional assumption of no axial motion

of the cable, then $\ddot{Y}$ vanishes. Under this circumstance, the rightmost term of (45) also vanishes. The equations now govern the torsional, vertical, and transverse (wind direction) motions of the cable. This particular set of circumstances was treated by Thompson (1975). The simplification of (36) and (37) agrees with his analysis. In Thompson's constitutive model, the parameter B is zero.

Absence of Ice. If there is no ice attached to the cable, then the center of the conductor and the center of mass of the cable cross-section coincide. The vector $\mathbf{r}_{cm}$ vanishes, and under this condition the equations of motion become

$$m\ddot{\mathbf{R}} = \mathbf{F}_{\text{aero}} + m\mathbf{g} + \frac{\partial}{\partial s}\left(\frac{1}{1+\epsilon}\left[P\frac{\partial \mathbf{R}}{\partial s} - \left(\hat{\mathbf{X}}_1\mathbf{k}^T\frac{1+\epsilon}{(X_s^2+Y_s^2)^{1/2}} - \hat{\mathbf{Z}}_2\hat{\mathbf{X}}_1^T\right)\cdot(I\alpha+\omega\times(I\omega))\right]\right) \quad (47)$$

and

$$(I\alpha+\omega\times(I\omega))\cdot\mathbf{e}_t = M_{\text{aero}} + \frac{\partial T}{\partial s}. \quad (48)$$

The remarkable aspect of (47) and (48) is that the torsional motion and the vertical motion are coupled together. It was previously believed that in the absence of ice, the torsional motion would uncouple from the translational motion, since in the work of Nigol and Havard (1978), it was noticed that the torsional frequency of vibration aligned with the translational frequency after ice had accumulated on the cable.

An important simplification occurs in the absence of both ice and torsional motion. Under this additional condition (47) becomes

$$m\ddot{\mathbf{R}} = \mathbf{F}_{\text{aero}} + m\mathbf{g} + \frac{\partial}{\partial s}\left(\frac{P}{1+\epsilon}\frac{\partial \mathbf{R}}{\partial s}\right) \quad (49)$$

which was originally presented by Shea (1955) and by Simpson (1963).

Ice-Free, Shallow Catenary Torsional Motion. Under these conditions, the moment balance expressed in (48) becomes

$$I\ddot{\theta} = M_{\text{aero}} + \frac{\partial T}{\partial s}. \quad (50)$$

Simpson (1972) presented the torsional equation for a bundled conductor. According to Simpson, the torsional moment attributed to stiffness is

$$M_T = \frac{\partial}{\partial s}\left(\frac{JG}{1+\epsilon}\frac{\partial \theta}{\partial s}\right) \quad (51)$$

where no elastic axial-torsional coupling is assumed. Equation (51) is true for Simpson's analysis regardless of the number (even one) of conductors making up the bundle. In comparing (51) with the work presented here, namely,

$$M_T = \frac{\partial}{\partial s}\left(JG\frac{\partial \theta}{\partial s}\right) \quad (52)$$

we see that the difference is a factor of $1/(1+\epsilon)$. By including the $1/(1+\epsilon)$ factor in the constitutive Eqs. of (10) and (11), rederiving the equations of motion, and invoking the same assumptions which lead to (50), the equations of motion as presented by Simpson are not recovered. There were additional terms not included in Simpson's analysis. It was found that only by using the constitutive model of (10) and (11) were we able to determine a result which was consistent with the virtual work analysis.

Conclusions

Equations of motion on a thin cable consisting of several wound strands subject to aerodynamic and eccentric mass loading have been derived. The equations of motion have been verified through a virtual work argument. By invoking suitable assumptions, simplifications of the presented work were shown to be in agreement with the work of previous investigators.

The equations of motion for the case where no ice is attached to the conductor demonstrated that the translational and torsional modes remained coupled. The presence of the coupling has not been known until now. In the galloping literature there is disagreement as to the initiating mode for galloping; i.e., does the instability stem from the torsional or vertical mode? The level of this disagreement is clearly seen in the two papers delivered by Nigol and Buchan (1981) and the following discussion. Nigol and his co-workers have demonstrated that given a conductor-ice geometry which is Den Hartog stable, an unstable system can be created by introducing a torsional oscillation. A significant contribution of the present work is that it provides a new direction for studying the various sources of mechanical instability which may be present in an iced conductor geometry.

Acknowledgments

The work presented here grew out of a study which was supported by Louisiana Power and Light Company. The authors wish to recognize LP&L and the Mechanical Engineering Departments of Kansas State University and Tulane University for their generous support of this work.

References

Cheers, F., 1950, "A Note on Galloping Conductors," Report No. MT-14, National Research Council of Canada, Ottawa, Canada.

Den Hartog, J. P., 1932, "Transmission Line Vibration due to Sleet," *Transactions of the American Institute of Electrical Engineers*, Vol. 51, pp. 1074–1076.

Gawronski, K. E., 1977, "Non-linear Galloping of Bundle-Conductor Transmission Lines," Ph.D. Dissertation, Clarkson College of Technology.

McConnell, K. G., and Zemke, W. P., 1976, "The Measurement of Flexural Stiffness of Multistranded Electrical Conductors While Under Tension," ERI Rep. No. 79194, Eng. Res. Inst., Iowa State University, Ames, Iowa.

Nigol, O., and Havard, D. G., 1978, "Control of Torsionally-Induced Conductor Galloping with Detuning Pendulums," IEEE Power Engineering Society Paper No. A78 125-7.

Nigol, O., and Buchan, P. G., 1981, "Conductor Galloping: Part I, Den Hartog Mechanism," *IEEE Transactions on Power Apparatus and Systems*, PAS-100, pp. 699–707.

Nigol, O., and Buchan, P. G., 1981, "Conductor Galloping: Part II, Torsional Mechanism," *IEEE Transactions on Power Apparatus and Systems*, PAS-100, pp. 708–720.

Routh, E. J., 1905, *A Treatise on the Dynamics of a System of Rigid Bodies, Part II*, 6th ed., Macmillan and Co., London, U.K., pp. 407–408.

Shea, J. F., 1955, "A Study of Wind Forces on Suspended Cables and Related Structures," Ph.D. Thesis, University of Michigan, Ann Arbor, Mich.

Simpson, A., 1963, "Oscillations of Catenaries and Systems of Overhead Transmission Lines," Ph.D. Thesis, University of Bristol, Bristol, U.K.

Simpson, A., 1972, "Determination of the Natural Frequencies of Multiconductor Overhead Transmission Lines," *Journal of Sound and Vibration*, Vol. 20, No. 4, pp. 417–449.

Thompson, H. A., 1975, "Galloping Vibration of Transmission Line Conductors Under Icing Conditions—Final Report," prepared for Louisiana Power and Light Co., Tulane University, New Orleans, La.